Supporting Information

Highly Efficient Photocatalytic Hydrogen Evolution Based on Conjugated Molecular Micro/nano-crystalline Sheets

Yuejuan Wan,[a] Jian Deng,[a] Cheng Gu[ab] and Yuguang Ma*[ab]

[a]*State Key Laboratory of Luminescent Materials and Devices, Institute of Polymer Optoelectronic Materials and Devices, South China University of Technology, No. 381 Wushan Road, Tianhe District, Guangzhou 510640, P. R. China.*

[b]*Guangdong Provincial Key Laboratory of Luminescence from Molecular Aggregates, South China University of Technology, Guangzhou 510640, P. R. China.*

Corresponding Author

E-mail:

*ygma@scut.edu.cn.

Materials

Benzo[1,2-b:5,4-b']dithiophene, 2-phenylacetonitrile, 6-bromonicotinaldehyde, n-butyllithium (n-BuLi), tributyltin chloride (Bu_3SnCl), tetrabutylammonium hydroxide (TBAH), trans-dichlorobis(triphenyl-phosphine)palladium (II) ($Pd(PPh_3)_4$), tetrahydrofuran (THF), dichloromethane (DCM), triethanolamine (TEOA), H_2O_2, H_2SO_4, methanol, acetone, ethanol, $CDCl_3$, DMF-d_7 were purchased from *Energy Chemical*. Chlorobenzene were purchased from *Sigma-Aldrich*. All the chemicals were used directly without further purification.

Dry air, N_2 (99.9999%) and Ar (99.9999%) were purchased form Mulai gas company.

Synthetic procedure

(Z)-3-(6-bromopyridin-3-yl)-2-phenylacrylonitrile: (1)

Benzyl cyanide (10.0 mmol, 1.2 mL) was added into a solution of 6-bromonicotinaldehyde (1.8500 g, 10.0 mmol) in methanol (100 mL) at 65 °C followed by TBAH (30% in methanol, 1.0 mL). After stirred 2 h, the reaction mixture was concentrated, washed with deionized water and hexane to get white needle-like solid with the yield of 70%. ^{1}H NMR (500 MHz, $CDCl_3$) δ = 8.60 (d, J = 2.5, 1H), 8.36 (dd, J = 8.4, 2.5, 1H), 7.69 (dt, J = 4.0, 2.2, 2H), 7.62 (d, J = 8.4, 1H), 7.51 – 7.44 (m, 4H). ^{13}C NMR (126 MHz, $CDCl_3$) δ = 151.48, 143.59, 136.71, 136.42, 133.48, 130.07, 129.30, 129.00, 128.46, 126.10, 117.17, 115.10. APCI MS: calcd. for $[M]^+$, m/z = 285.14; found m/z = 284.9.

Benzo[1,2-b:5,4-b']dithiophen-2-yltributylstannane and (Z)-3-(6-(benzo[1,2-b:5,4-b']dithiophen-2-yl)pyridin-3-yl)-2-phenylacrylonitrile: (2 and 3)

Under argon atmosphere, n-BuLi (2.5 M in hexanes, 0.52 mL, 1.30 mmol) was added slowly to a solution of benzo[1,2-b:5,4-b']dithiophene (0.1140 g, 0.6 mmol) in THF (15 mL) at -78 °C. After stirred for 30 min and then warmed to -25 °C, tributyltin chloride (1.2 mmol, 0.32 mL) was injected, and the solution was gradually warmed to 25 °C and stirred for 12 h. The crude residue was obtained after removing the solvent

under reduced pressure, dried with $MgSO_4$ as light yellow oil. Because the crude product was easily decomposed to the raw material, we could not get the purified product with definite NMR signal, just dried it and conducted the next step as soon as possible.

A mixture of benzo[1,2-b:5,4-b']dithiophen-2-yltributylstannane (0.4790 g, 1.0 mmol)and (Z)-3-(6-bromopyridin-3-yl)-2-phenylacrylonitrile (0.2851 g,1.0 mmol) was dissolved in 1,4-dioxane (15 mL). Under argon atmosphere, $Pd(PPh_3)_4$ (0.0046 g, 0.04 mmol) was added to the solution with reflux for 24 h. After cooling down to the room temperature, the solvent was removed under reduced pressure. The mixture was washed by water and ethanol for twice and then filtered. Because of the poor solubility of PCPyBDT in comment solvents, the crude product was purified by sublimation for twice to get yellow crystalline powder ultimately with the yield of 45%. ^{1}H NMR (500 MHz, DMF-d_7) δ = 9.14 (d, J = 2.1, 1H), 8.63 (dd, J = 8.5, 2.2, 1H), 8.50 (s, 1H), 8.46 (s, 1H), 8.41 (d, J = 8.5, 1H), 8.28 (s, 3H), 8.23 (s, 1H), 7.82 (d, J = 5.5, 1H), 7.53 (dd, J = 13.4, 7.2, 4H). Because of the poor solubility in common solvents, we could not get any signal for ^{13}C signal. APCI MS: calcd. for $[M]^+$, m/z = 394.51; found m/z = 394.1. Elemental analysis: calcd. for $C_{24}H_{14}N_2S_2$: C, 73.07; H, 3.58; N, 7.10; S, 16.25. found: C,72.56; H, 3.79; N, 7.56; S, 16.09.

Methods

^{1}H NMR and ^{13}C spectra were recorded on a Bruker AVANCE HD III 500 and 126M NMR spectrometer, respectively. Mass spectrometry data of compounds were obtained on a Waters ACQUITY TQD liquid chromatograph-mass spectrometer using APCI ionization. Elemental analysis was performed on a Flash EA 1112, CHNS-O elemental analyzer. TG measurements were performed on a PerkinElmer Thermal analysis under N_2, by heating to 800 °C at a rate of 10 °C min^{-1}. DSC measurements were performed on a NETZSCH (DSC-204) unit at a heating rate of 20 °C min^{-1} under N_2. X-ray diffraction (XRD) data were recorded on an XtaLAB P200 FR-X. UV-vis spectra were recorded on a Shimadzu UV-3600 spectrometer. Photoluminescence spectra were recorded on a Shimadzu RF-5301PC spectrophotometer. Transient

fluorescence spectra were measured on a FLS920 transient spectrometer. The raw data were processed with the Nanoscope analysis software. Optical images were recorded through Leica fluorescence microscope with DM4000 excitation at 340 to 380 nm. The optical waveguide measurement was performed by the third harmonic of a passively Q-switched Nd:YAG laser with a pulse width of 7 ns and the repetition of 20 Hz. The PL spectra were recorded by the fiber optical spectrometer with Ocean Optics QE Pro at resolution rate of 1 nm accompanied with the Nikon microscope. Cyclic voltammetry was recorded in a standard three-electrode electrochemical cell attached to a CHI 670C electrochemical workstation at a scan rate of 50 mV s^{-1}. The glass carbon electrodes coated with the powders were infiltrated into anhydrous acetonitrile or dichloromethane with 0.1 M $TBAPF_6$ as supporting electrolyte. Fourier transform Infrared (FT-IR) spectra were recorded on a VERTEX 80 V Fourier transform infrared spectrometer with KBr as reference. The potentials were measured against an Ag/Ag^+ reference electrode with ferrocene as internal standard. The photocatalytic reaction was conducted with 300 W Xe-lamp.

Optical waveguide measurement

The optical waveguide PL spectra with changed excited spot (λ_{ex} = 351 nm) were recorded for sheet-like crystal of PCPyBDT. After cleaning the quartz plates, the sheet-like crystals after careful selection were tightly pasted to the surface of quartz plates. The distance-dependent intensity was tested by the fiber optical spectrometer. The optical loss value α was fitted by the equation: $I_{tip} / I_{body} = A \exp(-\alpha d)$, where the A is a constant, and the D is the distance between the excited spot (body) and the emitting spot (tip), I_{tip} is PL intensity of signal collected spot and I_{body} is PL intensity of signal excited spot.

Cyclic voltammetry test

The electrochemical cyclic voltammetry (CV) test was applied to calculate the highest occupied molecular orbital (HOMO) and the lowest unoccupied molecular orbital (LUMO). A typical three-electrode cell worked with a working electrode (glass

carbon), a reference electrode (Ag/Ag^+, referenced against an internal standard of ferrocene/ferrocenium (FOC), and a counter electrode (Pt wire) in an acetonitrile or DCM solution of 0.1 M tetrabutylammonium hexafluorophosphate ($TBAPF_6$) as supporting electrolyte. We calculated the HOMO and LUMO energy levels based on the reference energy level of Ag/Ag^+ (-4.8 eV versus the vacuum level) according to the equations: $E_{HOMO} = -(Eox - E_{FOC}) - 4.8$ (eV), $E_{LUMO} = -(E_{red} - E_{FOC}) - 4.8$ (eV), where the value of E_{FOC} is the formal potential of FOC vs Ag/Ag^+ in special electrolyte solutions. The corresponding redox potential versus normal hydrogen electrode (NHE) could also obtained according to the reference standard for which 0 V versus NHE equals to -4.44 V. The reduction and the oxidation potentials are -1.30 V and 1.31 V for PCPyBDT, respectively. When the PH value was 11, according to Nernst equation, $E(H^+/H_2) = -0.059$ PH (V versus NHE), $E(O_2/H_2O) = E(H^+/H_2) - 1.23$ (V versus NHE), the reduction and oxidation potentials of water were -0.65 and 0.58 V, respectively.

Photocatalytic test

5 mg crystalline photocatalyst powder was grinded, and then added into the mixed aqueous solution (50 mL), including deionized H_2O (45 mL), chloroplatinic acid (20 μL, 8 wt% aqueous solution) as a Pt precursor, and TEOA (5 mL). After ultrasound 20 min, the photocatalyst powder was dispersed uniformly in aqueous solution. The mixture was degassed for 20 min to remove the air completely before irradiation with a 300 W Xe-lamp ($\lambda > 420$ nm) and cyclic condensation equipment. The generated hydrogen was detected by gas chromatography.

Apparent quantum efficiency measurement

The apparent quantum efficiency (AQE) of photocatalytic reaction was performed under irradiation of monochromatic light with different band-pass filters of 405, 420, 435, 450, 475 and 500 nm. The calculated equation was listed as follow:

$$AQE = \frac{n_e}{n_p} \times 100\%$$

$$n_e = 2n_{H_2} * N_A$$

$$n_p = \frac{E}{h\nu} = \frac{Pt}{h\nu} = \frac{Pt\lambda}{hc}$$

Where,

n_e: the number of reacted electrons during reaction process, in μmol;

n_p: the number of incident photons during reaction process, in μmol;

n_{H2}: the amount of generated hydrogen during reaction process, in μmol;

N_A: the Avogadro constant (6.022×10^{23} mol^{-1});

E: the photon energy under irradiation, in J;

h: the Planck constant (6.626×10^{-34} J s);

P: the power of incident light, in mW;

t: the reaction time, in hour;

λ: the incident wavelength, in nm;

ν: the frequency of incident light, in Hz;

c: the velocity of light (3×10^8 m s^{-1}).

Preparation and characterization of OFETs

The insulated surfaces of the silicon wafers were modified by polymethyl-methacrylate (PMMA) films with calculated capacitance per unit area (C_i) of 1.27×10^{-8} F cm^{-2} when the thickness of 80 nm. The sheet single crystals were tightly pasted to the surface of the PMMA-modified silicon wafers with the assistance of the electrostatic interaction. The CsF (MoO_3) with 2-nm thickness on the surface of sheet single crystal was used as the electron (hole) modification layer between crystals and Ca (Au) to improve the electron (hole) current. The symmetric Ca (Au) electrodes were deposited with the rate of 0.6 nm s^{-1} by controlling the channel length of 50 or 100 μm. The actual channel width (W) and length (L) were measured by optical microscopy. the chamber pressure was always remaining below 1×10^{-4} Pa during the deposition process. The subsequent measurement of electrical performance was conducted in the glove box by the semiconductor analyzer (Agilent Technologies B1500A and Keithley

2636B), in which both the concentration of the water and oxygen maintaining below 0.1 ppm, respectively.

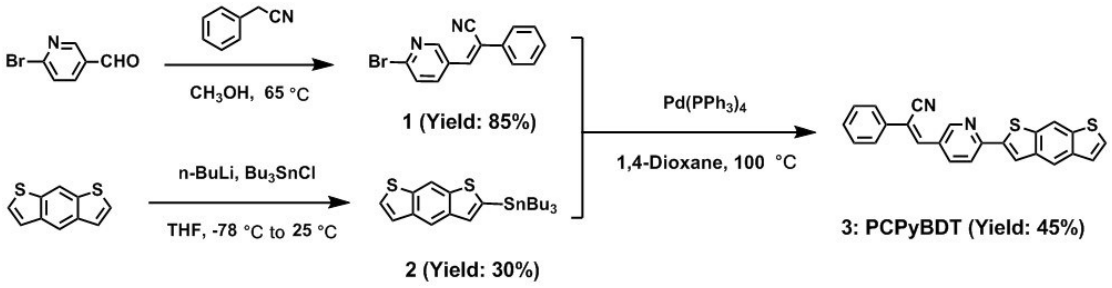

Scheme S1 The synthetic route of PCPyBDT.

Supporting Tables

Table S1 Crystallographic data and structural refinement summary for PCPyBDT crystal.

Compounds	PCPyBDT
empirical formula	$C_{24}H_{14}N_2S_2$
formula weight	394.49
Temperature (K)	101
crystal system	triclinic
space group	P-1 (2#)
a (Å)	5.99462(12)
b (Å)	14.5822(2)
c (Å)	20.4735(3)
α (°)	97.8257(12)
β (°)	94.0644(13)
γ (°)	95.0011(14)
V (Å^3)	1760.05(5)
Z	4
ρ_{calc} (g cm^{-3})	1.489
μ (mm^{-1})	2.83
diffractometer	CCD
F(000)	816
radiation type	Cu $K\alpha$
radiation wavelength (Å)	1.54184
goodness-of-fit on F^2	1.037
number of reflections collected/unique	5306/6174
R_{int}	0.0483
R_1 ($I > 2.00\sigma(I)$)[a]	0.0415
wR_2 ($I > 2.00\sigma(I)$)[b]	0.1116
CCDC number	1948360

[a]$R_1 = \Sigma||F_o|-|F_c||/\Sigma|F_o|$, [b]$wR_2 = [\Sigma w|F_o^2-F_c^2|^2/\Sigma w(F_o^2)^2]^{1/2}$

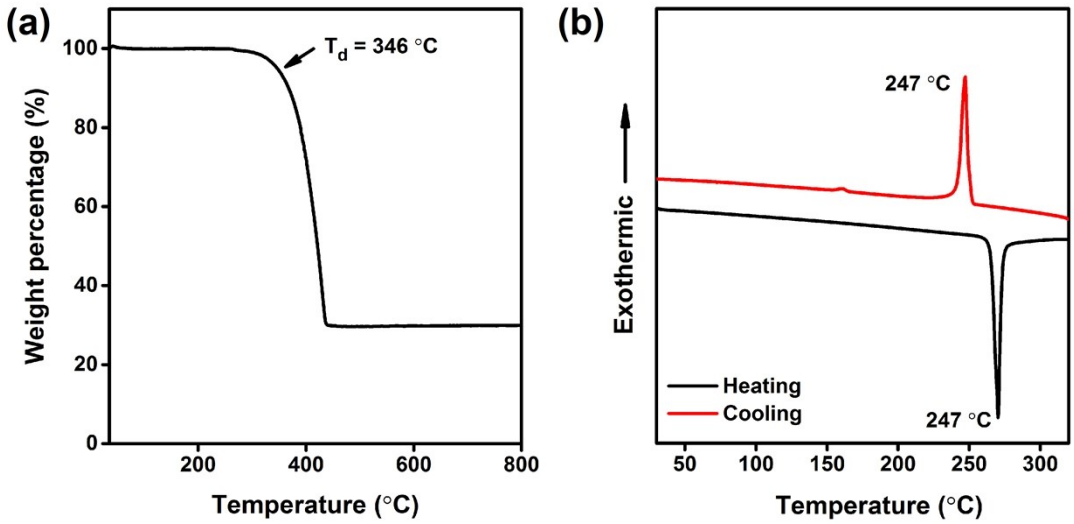

Figure S1 (a) TG and (b) DSC curves of PCPyBDT, showing that the decomposition temperature and melting point are 346 °C and 247°C, respectively.

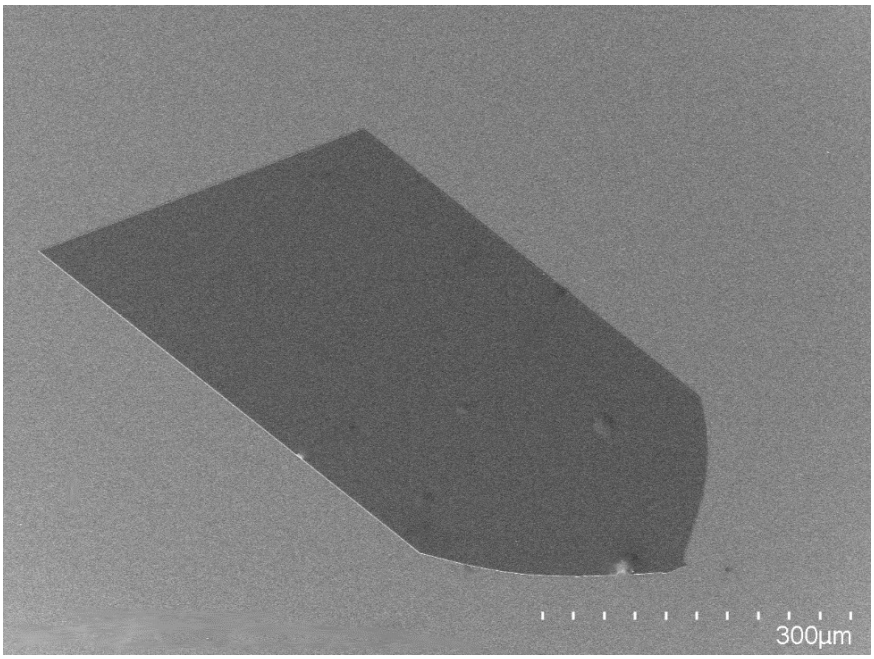

Figure S2 The SEM image of single crystal for PCPyBDT through physical vapor transport method.

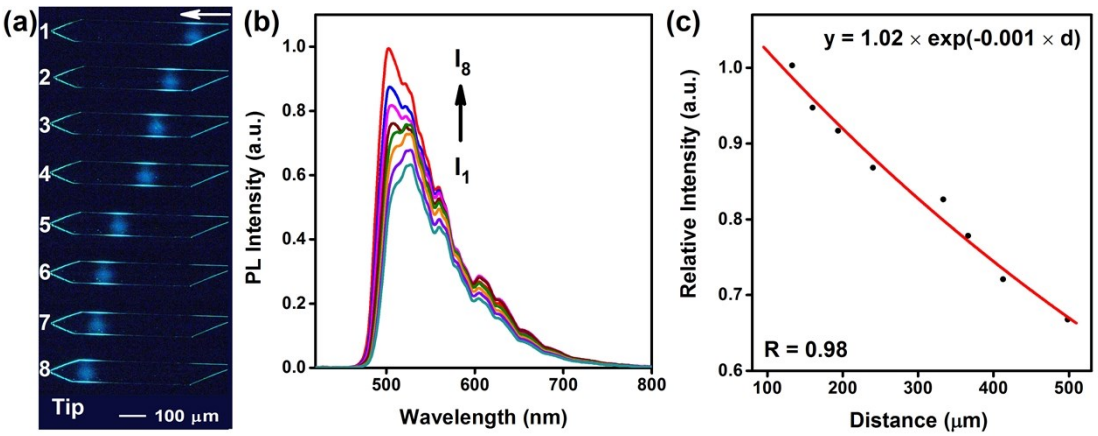

Figure S3 The optical waveguide measurement of PCPyBDT crystals: (a) the fluorescence images under changed excited laser spots; (b) the recorded PL spectra from the left of crystal; (c) the fitted optical loss value according to the equation: $I_{tip} / I_{body} = A \exp(-\alpha d)$, the fitted $\alpha = 0.001$ μm^{-1}.

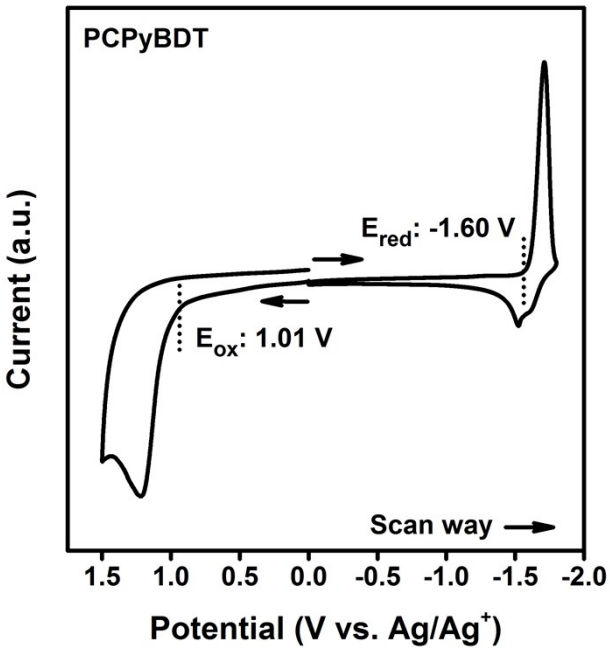

Figure S4 Electrochemical cyclic voltammetry measurement of PCPyBDT. According to the redox potential versus Ag/Ag^+, the calculated HOMO and LUMO were -3.14 and -5.75 eV for PCPyBDT.

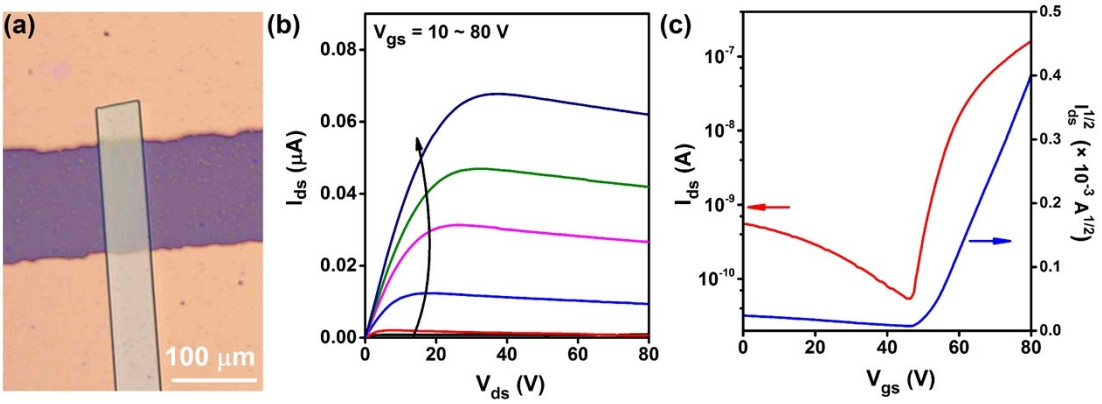

Figure S5 The electron transport characteristics based on single-crystal field-effect transistors with PMMA as dielectric layer, Au as symmetric electrodes and MoO_3 as hole buffer layer: (a) the photo of field-effect transistor device; the typical n-type (b) output and (c) transfer curves for PCPyBDT single crystal. There is not any hole transport signal and the calculated electron mobility is 0.09 cm^2 V^{-1} s^{-1}.

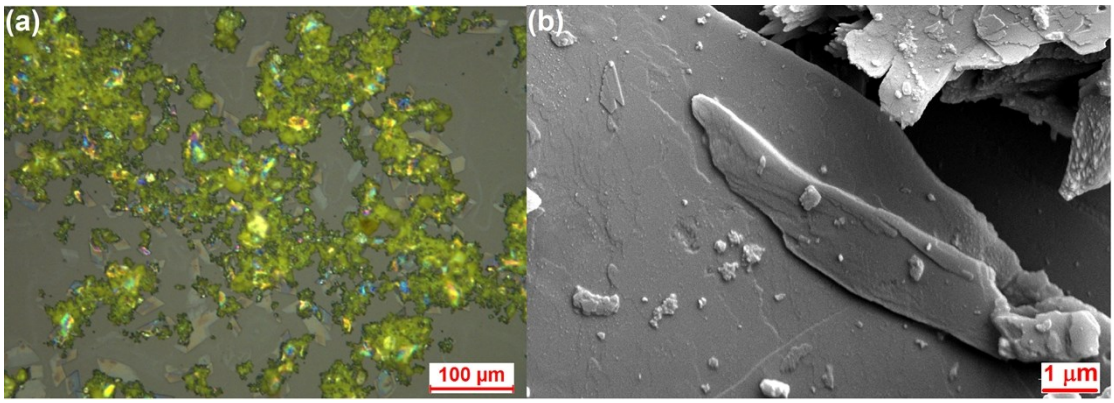

Figure S6 (a) The optical image under the natural light and (b) SEM image of dispersive micro/nano-sheets after grind for PCPyBDT. The crystalline sheets after sublimation were grinded to smaller-size micro/nano-sheets, then dispersed in the ethanol solution. The dispersed suspension solution after ultraphonic process were dropped on the quartz plates. After the ethanol was evaporated, we got the photos through optical microscope and SEM, respectively.

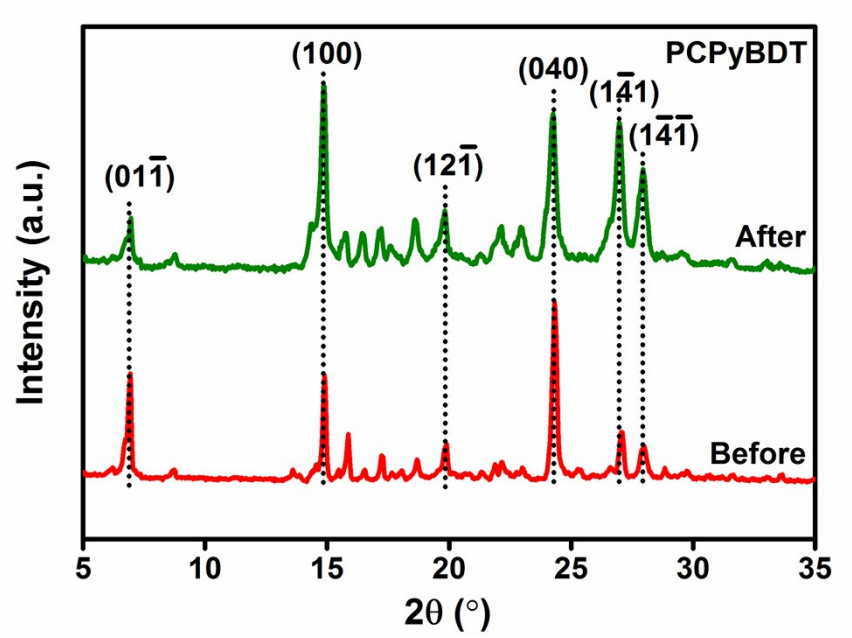

Figure S7 XRD patterns before and after photocatalytic reactions for PCPyBDT micro/nano-sheets.

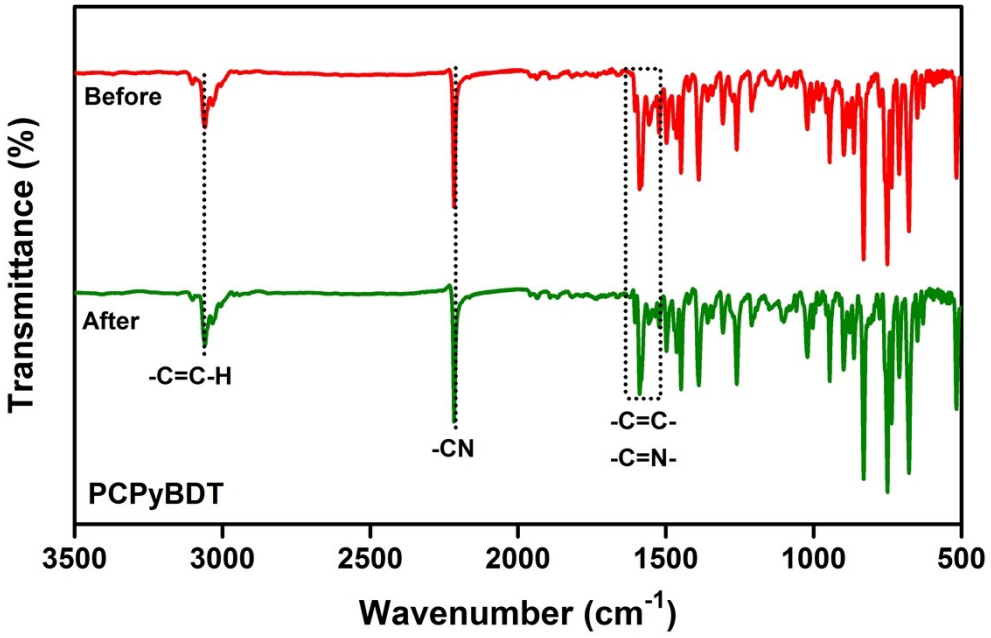

Figure S8 FTIR spectra before and after photocatalytic reactions for PCPyBDT micro/nano-sheets.